scientific reports

Check for updates

OPEN

Research on curing reaction kinetics and curing process of hydroxy-terminated polybutadiene (HTPB) propellants

Zhiming Guo[1,2], Yiliang Wang[3], Michele Chiumsenti[1], Yuheng Wu[3], Shaocong Zhen[3], Hanwen Liu[3], Riccardo Rossi[1] & Xiaolong Fu[3]✉

Hydroxyl-terminated polybutadiene (HTPB) propellants are high-performance solid propellants widely used in aerospace and military applications. By combining experimental and theoretical approaches, the curing process was analyzed using differential scanning calorimetry (DSC) to obtain reaction data at various heating rates. A thermochemical model and a finite-element model were developed to simulate the curing process, revealing the evolution of temperature and curing degree. The results indicate that higher heating rates significantly accelerate the curing reaction, reducing the curing time. The close agreement between the simulation and experimental data validates the reliability of the model. Future work could expand the model to include additional practical factors, such as material impurities and complex working conditions, to further optimize the HTPB propellant curing process.

Keywords HTPB propellant, Curing process, DSC, Thermochemical model, Finite element analysis

Hydroxyl-terminated polybutadiene (HTPB) propellants are widely recognized as high-performance solid propellants. They are composed of metallic fuel, inorganic oxidizers, HTPB binder, curing agents, and plasticizers[1,2]. Functioning as a polymeric binder, HTPB integrates heterogeneous raw materials into a homogeneous matrix. It exhibits exceptional high energy density, stable structure, chemical stability, and good processability[3]. These attributes have made HTPB propellants indispensable in aerospace and defense applications, driving advancements in propulsion technologies[4]. Among the critical stages in propellant manufacturing, the curing process significantly determines the final mechanical and thermochemical properties of the product[5]. Therefore, the study of the curing process is crucial for the wider application of HTPB propellants in aerospace and defense fields.

In order to investigate the impact of the curing process on propellant properties, numerous scholars have utilized simulation and DSC experimental methods to explore the optimization of curing parameters. For example, Moghimi Rad et al.[6] developed a computational solver (CureFOAM) based on OpenFOAM to analyze the temperature-dependent curing kinetics of HTPB resin. The results showed a maximum relative error of 5% compared to experimental data. Similarly, Chen et al.[7] studied the multi-physical field effects during the curing of nitrate ester plasticized polyether (NEPE) propellants, correlating residual stress distributions with thermal and chemical gradients. Liu et al.[8] investigated the mechanisms of residual stress and strain formation in nitrate ester plasticized polyether (NEPE) propellant grains through numerical simulations. Using the ABAQUS finite element (FE) platform, they systematically examined the temperature evolution, curing degree, and stress/strain distributions during the curing and cooling phases.

Abraham Varghese et al.[9] discovered that the reaction levels differed between the pre-gel and post-gel stages. By measuring the viscosity and torque changes during the reaction between HTPB and TDI, they found that the reaction rate of the system was influenced by the mole fraction of trifunctional hydroxyl groups and the amount of small-molecule alcohols added. This finding is crucial for controlling the curing process and determining the applicability period of HTPB propellant. Sangmook Lee et al.[10] employed DSC and a rheometer to study the curing reaction of HTPB with IPDI. They determined the activation energy of the reaction and constructed the master curve, providing a basis for predicting key information in the manufacturing process of polymer-bonded explosives and HTPB propellants.

[1]Departament d'Enginyeria Civil i Ambiental (DECA), Universitat Politécnica de Catalunya (UPC), Jordi Girona 1, Barcelona 08034, Spain. [2]School of Mechatronics Engineering, North University of China, Taiyuan 030051, China. [3]Xi'an Modern Chemistry Research Institute, Xi'an 710065, Shaanxi, China. ✉email: fuxiaolong204@163.com

Ma Hui et al.[11] compared the effects of different catalysts on the curing reaction of the HTPB-IPDI system using DSC and viscosity tests. They concluded that DBTDL has high catalytic activity but a short application period, while TECH has low toxicity and a long application period. This research provides a reference for choosing a suitable curing catalyst for HTPB propellant. L.T. DeLuca et al.[12] characterized HTPB-based solid fuels in terms of performance, mechanical properties, and pollution through the design of burner experiments, etc. They found that HTPB has issues such as a low regression rate and explored strategies to enhance the performance of HTPB propellant by adding high-energy metal additives, which is of great significance for improving the performance of HTPB propellant.

Jiahu Guo et al.[13] used FT-IR spectroscopy to study the curing reaction between HTPB and IPDI and determined the kinetic parameters and the two-step reaction mechanism, which aids in understanding the curing process of polyurethane in HTPB propellant. Hui Ma et al.[14] investigated the curing reaction of HTPB and HDI-trimer with different catalyst mass fractions through rheological dynamics and obtained the relationship between the applicable period of the system and the catalyst mass fraction. This provides theoretical guidance for controlling the applicable period of the curing system of HTPB propellant. They also[15] investigated the effect of different curing agents on the curing reaction of HTPB-based adhesive systems using the viscosity testing method. They determined the rheological reaction rate constants and the applicable period of different systems and found that the viscosity of the HDI-trimer-cured HTPB system increased rapidly in the later stage, which is beneficial for improving the final performance of the product in the manufacturing process of HTPB propellant.

Xing Zhang et al.[16] investigated the curing reaction and performance of EHTPB-IPDI and HTPB-IPDI systems using DSC, viscosity tests, and a universal testing machine. They found that the EHTPB-IPDI system is more reactive during curing, and its cured product has better thermal stability and mechanical properties, which is more advantageous in the application of HTPB propellant. Also, DBTDL has a better catalytic effect on this system than TECH. Jie Zhou et al.[17] investigated the polyurethane moisture-curing reaction using in-situ FTIR spectroscopy and DFT calculations. The results showed that the reaction initially followed one-stage reaction kinetics. The increase in humidity and temperature accelerated the reaction process, and additional water molecules acted as catalysts for the reaction, providing theoretical references for understanding the polyurethane curing process in HTPB propellants.

Ehtasimul Hoque et al.[18] explored the curing kinetics of 4 - (dimethylsilyl) butylferrocene - grafted HTPB with the aid of DSC, viscosity tests, etc. They found that although the activation energy of this system was higher, the curing reaction rate was faster, and the catalytic effect of $Fe(AA)_3$ was better than that of DBTDL. This can help optimize the formulation design and the curing process of HTPB propellant. C. Korah Bina et al.[19] examined the curing reaction of HTPB with different isocyanates using DSC, viscosity tests, and FTIR spectroscopy. They found that the catalytic effect of FeAA on the curing reaction of HTPB was better, and the results of the viscosity tests were consistent with the DSC analysis, which is of great significance for the curing research and practical production of HTPB propellant. Despite these advancements, detailed investigations into HTPB propellant curing mechanisms remain limited.

This paper presents an analysis of the curing process using differential scanning calorimetry (DSC), combining experimental and theoretical approaches. Curing behavior was characterized at various heating rates, and the influence of heating rate on reaction kinetics was investigated. Kinetic parameters for the curing reaction were determined using the Kissinger and Ozawa methods. Furthermore, thermochemical and finite element (FE) models were developed to simulate the curing process, revealing the evolution of temperature and degree of cure. Validated by isothermal and adiabatic experiments based on thermally activated Arrhenius-type kinetics, the model explains the enhancement of rheological properties. This effectively bridges the gap between laboratory-scale observations and FE implementation requirements[20–23].

The paper is structured as follows: Sect. 2 details the experimental setup, including materials such as HTPB, ammonium perchlorate, and aluminum powder. The preparation of propellant slurries using a 5 L vertical planetary mixer is comprehensively described. Section 3 develops two theoretical models: (1) A thermochemical model that precisely defines the degree of cure and reaction rate, incorporating Arrhenius-type thermally activated kinetics and heat release during curing; and (2) A finite element (FE) modeling framework detailing the application of an FE solver for curing process simulation, covering software implementation, model geometry, and material thermophysical properties. Section 4 presents results and corresponding discussions. Based on non-isothermal DSC data, it analyzes the influence of heating rate on curing reaction kinetics. Activation energies and other kinetic parameters were calculated using the Kissinger and Ozawa methods. Simulation results are compared with experimental data, with temperature and degree of cure evolution investigated at different nodal positions during curing. Section 5 summarizes the study, confirming that heating rate significantly affects curing reaction kinetics, thereby validating the model. Future work may extend the model by incorporating additional practical factors to enhance process control.

Experiment setup

Material

The investigated propellant material consists of HTPB as the polymeric binder, along with ammonium perchlorate (AP) and aluminum powder (Al) as solid fillers. The basic formulation of the NEPE propellant is presented in Table 1. The molecular structures of HTPB, Dioctyl sebacate (DOS), and Toluene Diisocyanate (TDI) are shown in Fig. 1.

Propellant slurry preparation

The propellant slurry was synthesized in a 5 - L vertical planetary mixer equipped with dual counter - rotating blades that operated at 30 rpm. The formulation used a bimodal solid - loading system consisting of 78 wt% particulate components, namely aluminum fuel (with a particle size of 5 μm) and ammonium perchlorate

HTPB/%	DOS/%	AP/%	Al/%	TDI/%
14.1	7	60	18	0.9

Table 1. The propellant composition.

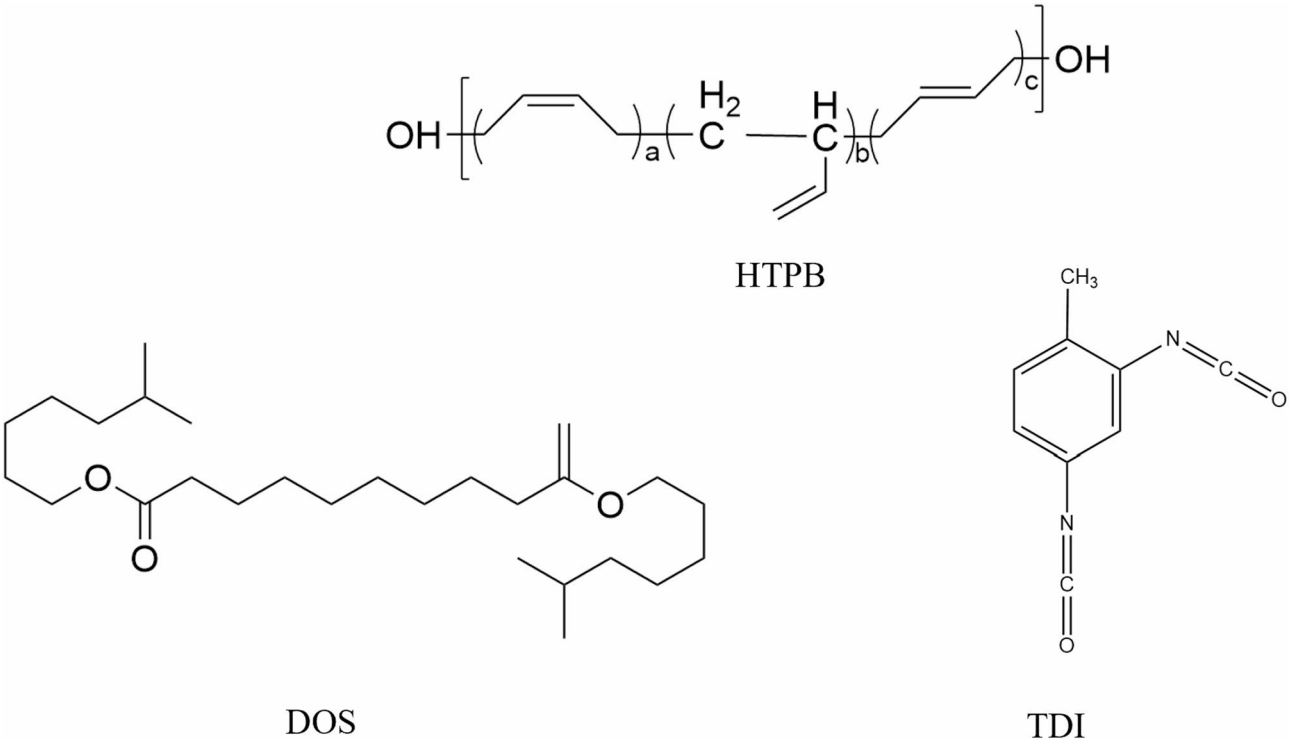

Fig. 1. Molecular structure of HTPB DOS and TDI.

oxidizer (the ratio of coarse - to - fine AP was 2:1, with D50 values of 120 μm and 7 μm respectively). The liquid phase, accounting for 22 wt%, was a polyurethane prepolymer system composed of HTPB, DOS plasticizer, and TDI curing agent. The mixer was configured with a thermal - management jacket, which maintained the slurry temperature at 323.15–333.15 K through regulated hot - water circulation.

Curing experiment

The prepared slurry was transferred into pillar-shaped molds and underwent thermal curing in a precision-controlled oven kept at a constant temperature of 323.15 K. As depicted in Fig. 2 (positions A–C), a triaxial thermal monitoring setup was adopted. T-type thermocouples were strategically placed at different geometric locations within the specimen. The thermopotential signals from the measuring end of the thermocouples were amplified by an amplifier, and the temperature at the reference end was detected by an integrated temperature sensor. The overall schematic of the isothermal curing system is illustrated in Fig. 3.

Thermal analysis was carried out using a DT-40 Differential Scanning Calorimeter (DSC). Specimens, weighing between 5.0 and 6.0 mg, were subjected to non-isothermal scanning from 293.15 K to 483.15 K at four heating rates, namely 5, 10, 15, and 20 $K{\cdot}min^{-1}$. This process helped in establishing a comprehensive thermal database for the optimization of the HTPB propellant formulation.

Non-isothermal DSC method

Thermal analysis of the samples was conducted using differential scanning calorimetry (DSC)[24]. The experiment was carried out in a high-pressure crucible with nitrogen as the ambient gas. To study the curing reaction kinetics of the samples, four different heating rates were set: 2.5 K/min, 5 K/min, 10 K/min, and 15 K/min. Throughout the experiment, the peak exothermic temperature of the sample at these four heating rates was recorded in real time by a precisely controlled temperature control system.

Theoretical models

Thermo-chemical model

The chemical processes that take place during the aging of polymers after they are cast are accompanied by substantial temperature variations. Consequently, the curing process is an exothermic and thermally activated reaction[25].

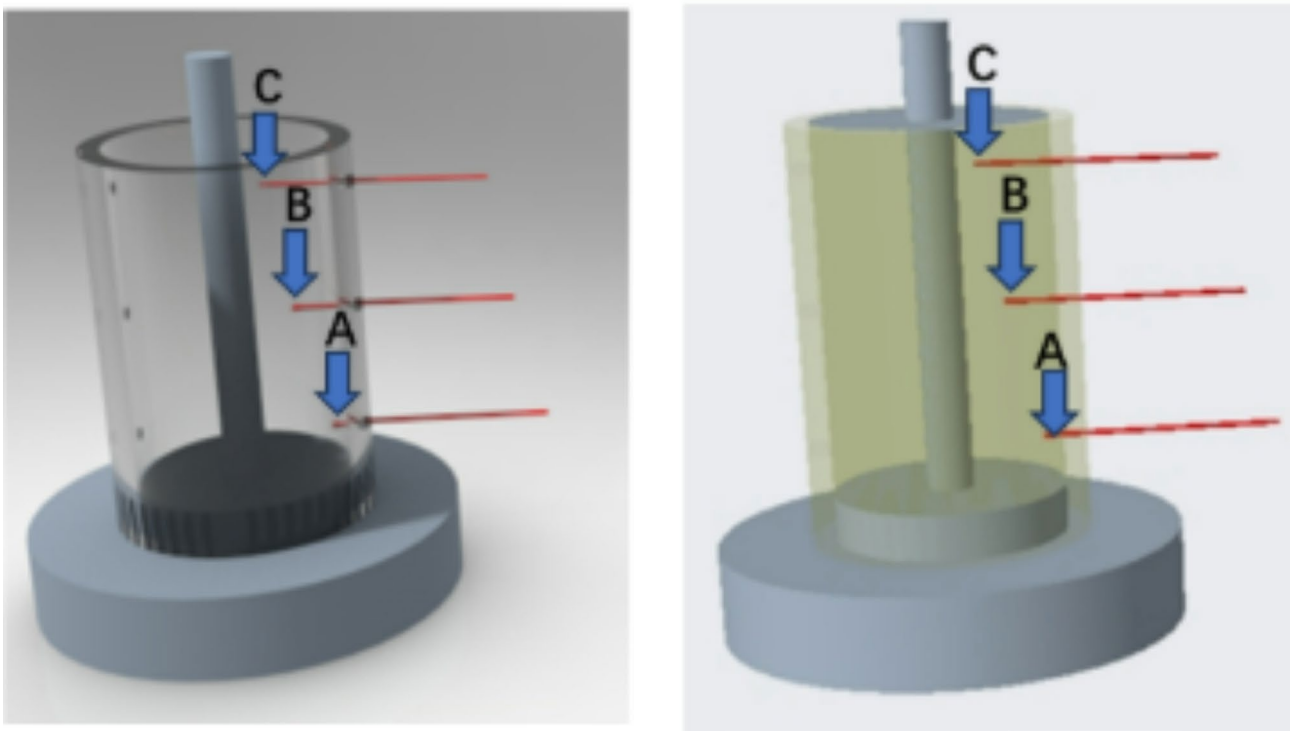

Fig. 2. T-Type thermocouple location distribution.

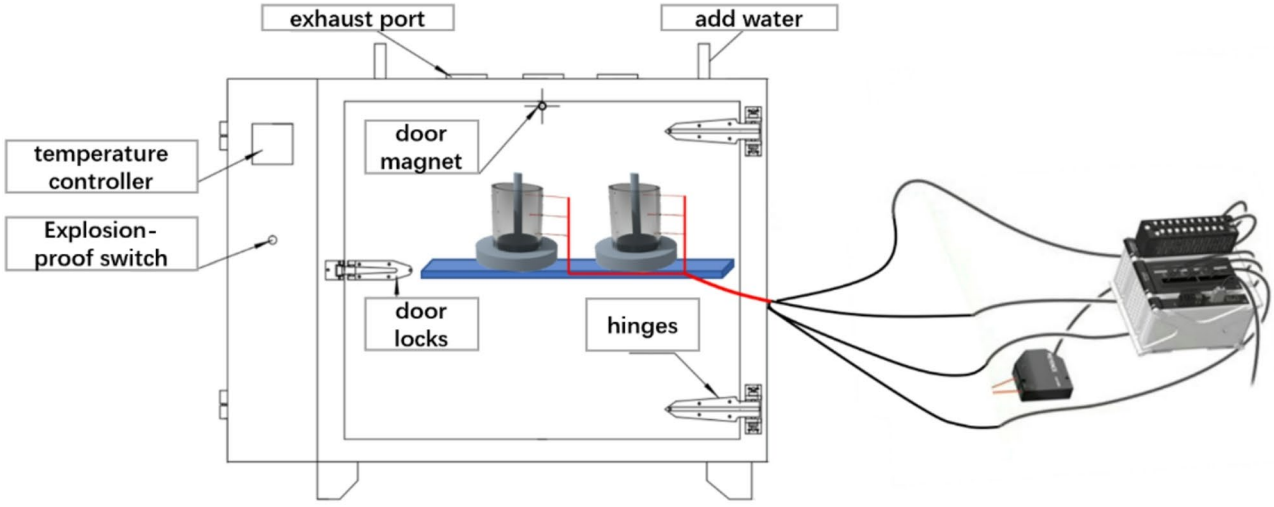

Fig. 3. Overall diagram of constant temperature curing system.

Since the kinetics of the reaction is determined by the curing agent concentration, χ, for more convenient handling and interpretation, the degree of curing, $0 \leq \zeta \leq 1$, is defined in the normalized format as:

$$\zeta = \frac{\chi}{\chi_\infty}, \tag{1}$$

where χ_∞ is the final value of χ (attained under perfect conditions). Thus, it can be hypothesized that the curing degree serves as the internal variable of the system, thereby indicating how far the kinetic reaction has progressed.

The reaction rate, denoted as $\dot{\zeta} = A(\zeta)$ is a characteristic feature of the kinetic reaction. Typically, it is a function of the curing degree ζ itself.

$$A(\zeta) = K_0(1-\zeta)(\zeta + \zeta_0), \tag{2}$$

where K_0 represents the chemical affinity, and ζ_0 corresponds to the value of the curing degree associated with the initial curing agent concentration χ_0, This correspondence ensures that the reaction initiates with an initial reaction rate $A(\zeta_0) \neq 0$. The proposed evolution law can be further refined by incorporating an exponential term, as illustrated in the following expression:

$$A(\zeta) = K_0(1-\zeta)(\zeta + \zeta_0) \cdot exp(-\delta\zeta), \tag{3}$$

where δ is a novel parameter of the model, which has the ability to predict the peak that corresponds to the maximum transformation rate. Consequently, the transformation process proceeds more rapidly at the onset of the curing process and slows down towards the end.

Kamal-Sourour proposed alternative models of the general form[26].

$$A(\zeta) = (K_1 + K_2\zeta^m)(1-\zeta)^n. \tag{4}$$

The curing process is also governed by thermally activated reactions. An Arrhenius-type law will be taken into account as well to explain its acceleration caused by the temperature field[27–29]. Therefore, the following formula is proposed for calculating the curing rate:

$$\dot{\zeta} = A(\zeta)\ exp\left(-\frac{E_a}{RT}\right), \tag{5}$$

where the Arrhenius exponential term includes the temperature *T*, the universal gas constant *R* for ideal gases, and the activation energy of the reaction E_a.

Upon examining this rate equation, it becomes clear that the thermal activation represented by the Arrhenius factor plays a crucial role at the initiation of the reaction. As the reaction progresses, significant attenuation is brought about by both the permeability exponential term and the factor $(1-\zeta)$, This results in the suppression of the reaction evolution as the curing degree approaches its final value $(\zeta = 1)$. Therefore, the kinetic equations, which must have positive values, incorporate the essential elements necessary for a realistic simulation of the kinetic reaction.

The curing reaction is typically characterized by the release of energy ($\dot{Q}_{reac}$) in the form of heat, which can be expressed as follows:

$$\dot{Q}_{reac} = L\dot{\zeta}. \tag{6}$$

The heat release during the curing reaction depends on the progression of the curing process, denoted as *L*, which represents the total heat released throughout the entire kinetic reaction. When the released heat is measured under adiabatic conditions, the proposed curing model can be readily calibrated by fitting the curve of the heat release evolution, as described below:

$$\zeta(t) = \frac{\Delta Q_{reac}(t)}{L}. \tag{7}$$

Finite element modeling

The curing process of HTPB propellant was simulated using a finite element solver. First, after integrating the curing interface, 3D modeling was carried out using the GID software tool or other CAD-supported software for propellant modeling, and an appropriate rendering mode was selected for the simulation.

The presented curing model has been tested with several geometries of interest, and the relevant data are presented in Table 2. The thermos-physical material properties are showed in Table 3. The 3D geometry model of the HTPB propellant depicted in Fig. 4a was ultimately chosen for this paper. The geometry of the HTPB propellant was discretized into 128,040 tetrahedral solid elements, as illustrated in Fig. 4b.

The solver type was set as DIRECT, the Time Increment was set to 60, the Number of Time Steps was set to 100, and the boundary function was defined as linear.

The thermos-physical material properties used for the simulation of all test cases are reported below:

Results and discussion

Curing reaction kinetics based on non-thermal DSC method

As shown in Fig. 5, the DSC curing reaction exhibits a smooth exothermic profile. It has been observed that the time needed for the curing reaction is remarkably shortened as the heating rate increases. Moreover, an upward trend in the onset, peak, and end temperatures of the curing process has been noted with the rise in the heating rate. This phenomenon can be attributed to the fact that a higher heating rate causes the molecular chains during

Type	Outer diameter (mm)	Length (mm)	Inner diameter (mm)
single hole tubular	50	50	5

Table 2. Geometric model No.1.

Parameter	Value	Unit
Density	1700	kg/m^3
Specific heat	1256	J/(kg K)
Heat conductivity	0.5	W/(m K)
Exothermic reaction heat	1.0e + 05	J/kg
Heat transfer by convection	25	W/(m^2 K)
Emissivity	0.6	–
Oven temperatures	333.15-353.15	K

Table 3. The thermos-physical material properties.

the curing process to be unable to arrange themselves rapidly enough according to the rules. Consequently, higher temperatures are required for the transition to the elastomeric state.

The curing reaction temperatures of the experimentally used patterns at different heating rates are depicted in Table 4.

In the table: β is the rate of temperature increase (K·min^{-1}); T_i is the starting temperature of the curing reaction during the test (K); T_p is the peak temperature of the curing reaction during the test (K); T_f is the ending temperature of the curing reaction during the test (K).

The principal approaches for ascertaining the activation energy of the curing reaction are the Kissinger method and the Ozawa method[28–30]. The Kissinger equation can be formulated as follows:

$$ln\frac{\beta}{T_p^2} = ln\frac{AR}{\Delta E} - \frac{\Delta E}{RT_p}, \tag{8}$$

where A is the curing finger front factor, (s^{-1}); ΔE is the reaction activation energy, (kJ·mol^{-1}); R is the molar gas constant, J/(mol·K).

Kissinger's method determines the activation energy of the curing reaction. It conducts a linear fitting with $1000/T_p$ as the abscissa and $\ln\frac{\beta}{T_p^2}$ as the ordinate. The activation energy of the curing reaction process is then derived from the slope of the resulting straight line obtained by the fit. Additionally, based on the value of the intercept, an estimate of the pre-exponential factor A can be obtained. Likewise, with the aid of Crane's equation[31], the number of reaction stages n in the curing reaction process can be determined. This is achieved by performing a linear fitting with $1000/T_p$ as the abscissa and $\ln\beta$ as the ordinate. The Crane equation is expressed as follows:

$$\frac{d\,(ln\beta\,)}{d(1/T_p)} \approx -\left(\frac{\Delta E}{nR}\right). \tag{9}$$

The fitting results are presented in Fig. 6. Based on the content of the figure, the calculated values are $\Delta E =$ 22.439 KJ·mol^{-1}, A = 33.779s^{-1} and $n = 0.8527$.

The Ozawa equation can be expressed as

$$log\beta = log\frac{A\Delta E}{Rf\,(\alpha\,)} - 2.315 - 0.4567\frac{\Delta E}{RT}, \tag{10}$$

where $f\,(\alpha\,)$ is the mechanism function of the inhomogeneous phase system.

According to the above equation, Ozawa's method is used to calculate the activation energy of the curing reaction by performing a linear fit. The activation energy of the curing reaction process is derived from the slope of the line obtained through the fit. The kinetic equations fitted by Ozawa's method are shown in Fig. 7. Similarly, with the aid of Crane's equation, the number of reaction stages n in the curing reaction process can be determined.

The kinetic parameters of the curing reaction process are shown in Table 5 below.

Temperature and curing degree during curing process

The curing temperature-time curves at various nodes of the experimental test conducted in an oven maintained at 323.15 K are illustrated in Fig. 8. Evidently, as indicated by the data, the temperature of the outermost layer is higher than that of the inner part, and the final temperature approaches the preset oven temperature. The curing process can be elaborated upon in three distinct stages.

In the initial stage, the temperature of the propellant samples rises rapidly during the curing process. This is predominantly attributed to the heat transfer from the interior of the oven and the exothermic characteristic of the propellant curing reaction. Specifically, the temperature reaches approximately 320.15 K at around the 4000-second mark.

During the second stage, the temperature within the solid propellant undergoes a gradual increase until it reaches a peak, followed by a slight decline. This phenomenon can be ascribed to the exothermic nature of the curing reaction. The rapid release of heat during the reaction, which is relatively low in comparison to the rate

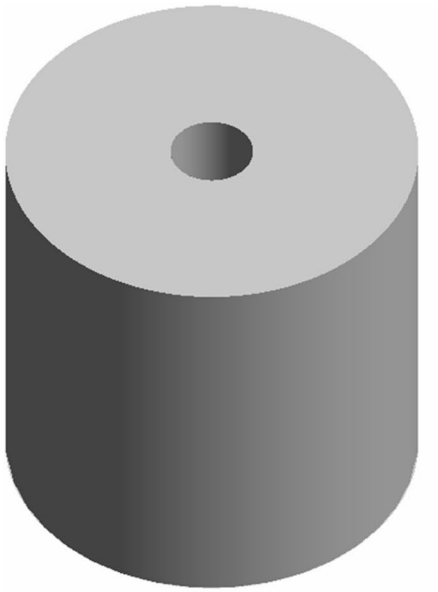

(a) Geometric model

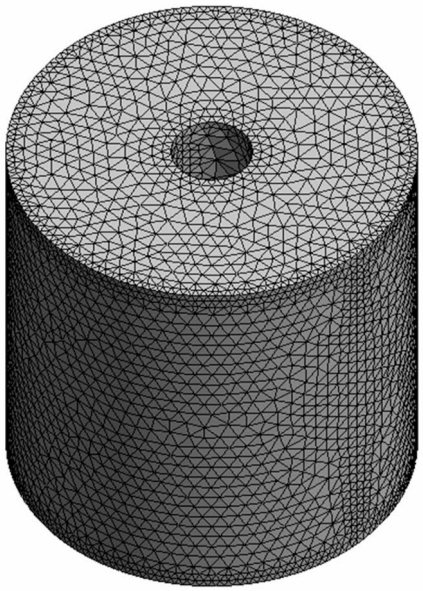

(b) Discrete mesh model

Fig. 4. 3D propellant model.

of heat transfer with the ambient environment, causes a slight decrease in temperature once the crosslinking reaction is completed.

In the final stage, owing to the stabilization of the ambient temperature, the internal temperature of the solid propellant gradually converges towards the external ambient temperature.

Figure 9 presents a comparison of the curing temperature - time profiles at different nodes during the curing experiments and the simulation process. It can be observed that the temperature - change experimental process at points A, B, and C is essentially similar to the simulation process. The maximum error in the comparison

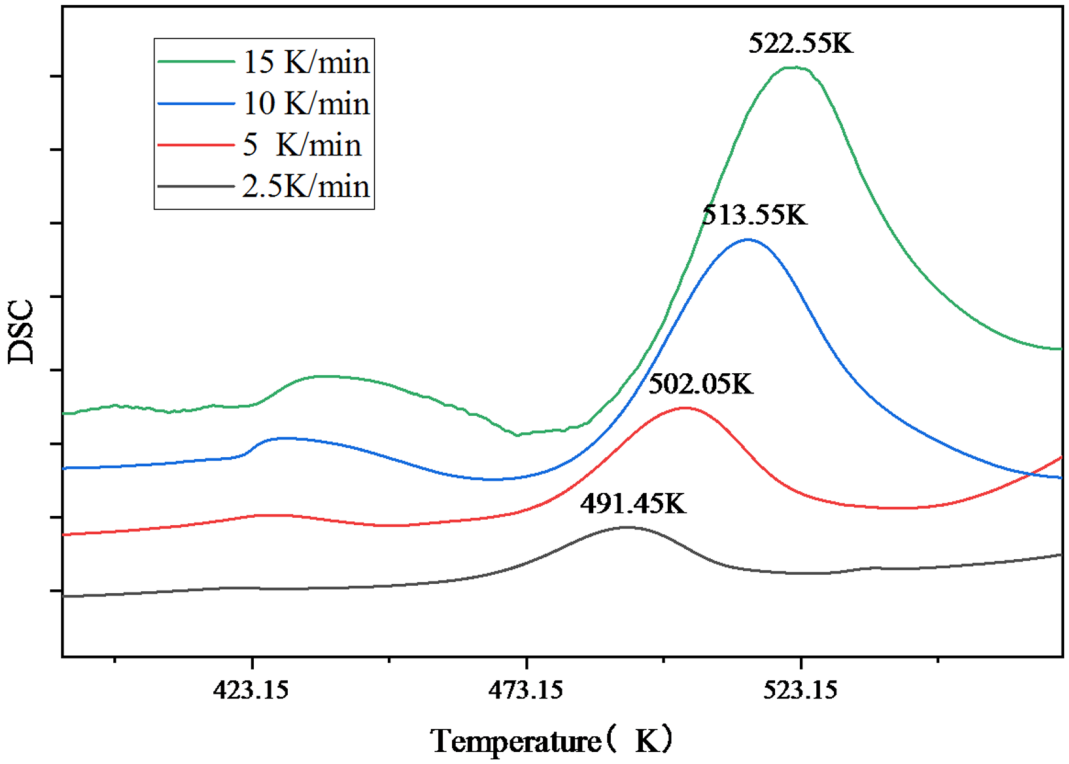

Fig. 5. The Y-axis offset stacked plot of the exothermic curve of DSC for the curing reaction.

β/K·min^{-1}	T_i/K	T_p/K	T_f/K
2.5	436.15	491.45	522.35
5	443.05	502.05	541.35
10	464.05	513.55	572.35
15	476.15	522.55	569.45

Table 4. Kinetic parameters of curing reaction.

between the experimental and simulation data for the three measurement points, as derived from the figures, is less than 5%. The 50 °C simulation is carried out based on the simulations at 333.15 K and 348.15 K, in line with the experimental results.

Analysis of simulation results

It is hypothesized that the experimental results under the 323.15 K condition are essentially consistent with the simulation outcomes. As a result, curing simulation experiments were carried out at 333.15 K and 348.15 K. As shown in Fig. 10, during the 323.15 K curing process, the temperature profile initially rises rapidly at the start of curing and then increases gradually due to a small amount of heat release until the curing is complete. Eventually, the temperature reaches 323 K, and the final temperature is identical at all measurement points. This is because, in the early stages of curing, the heat from the oven is rapidly transferred to the propellant sample, and the exothermic nature of the propellant curing reaction also contributes to the rapid temperature increase. As the reaction progresses, the exothermic rate of the reaction reaches an equilibrium with the ambient heat transfer rate, and the rate of temperature rise slows down until, at the end of curing, the temperature stabilizes around the set ambient temperature.

As depicted in Fig. 11, the curability curve commences to rise steadily and decelerates as it approaches the completion of curing. In the initial phase of curing, the curing agent reacts comprehensively with HTPB and other components. The curing reaction rate is high, leading to a rapid increase in the degree of cure. As the reaction progresses, the curing agent is gradually depleted, the number of unreacted active sites diminishes, the reaction rate declines, and the growth of the degree of cure slows down until curing is complete. At this point, the degree of cure attains its maximum value. The cloud diagram of the curing simulation process is shown in Fig. 12.

Figures 13 and 14 illustrate the temperature profile and cure degree change profile at 333.15 K. When curing at 333.15 K, the temperature trend is similar to that at 323.15 K. However, the maximum temperature after curing reaches 333 K, which is higher than that at 323.15 K. This is because, at higher temperatures, the molecular

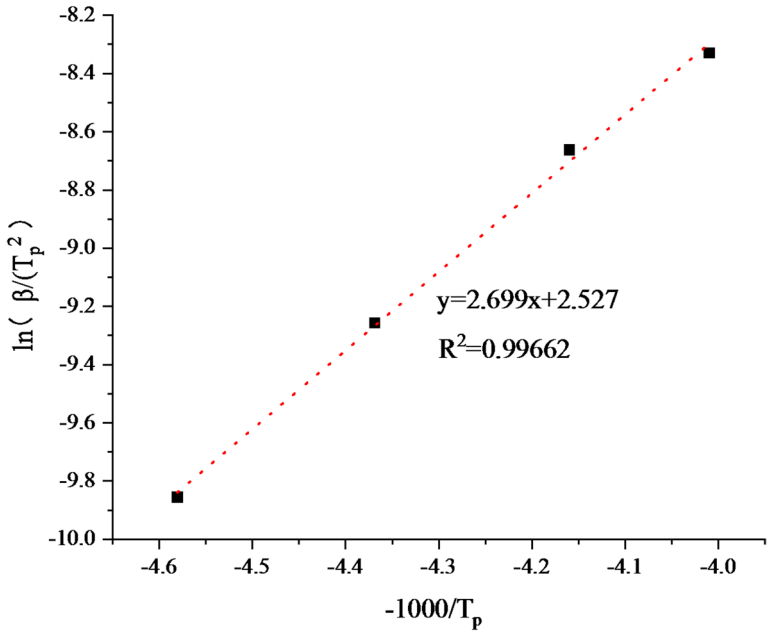

(a)

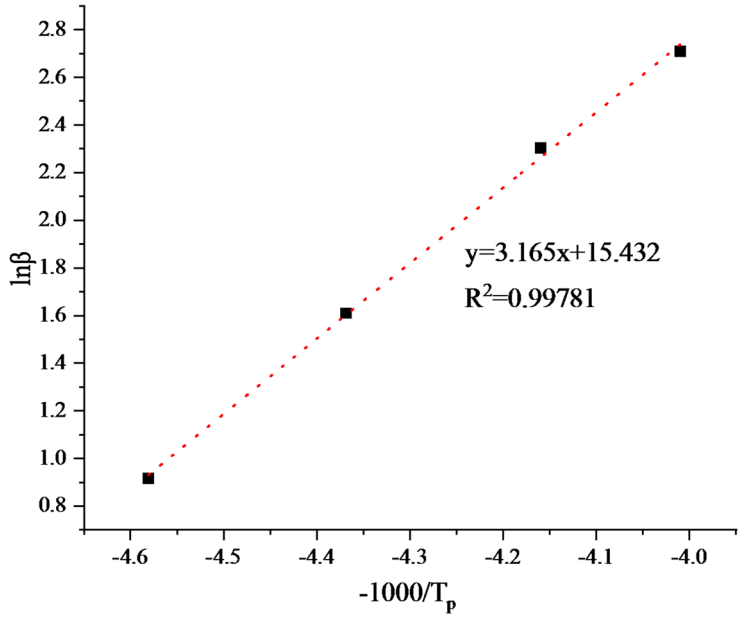

(b)

Fig. 6. Kissinger method for solving kinetic parameters.

thermal motion intensifies and the reactivity increases. As a result, the curing reaction rate accelerates. With a higher reaction rate, more heat is released within the same time interval. Consequently, the final temperature is higher.

According to the simulated cloud diagram in Fig. 15, it can be seen that the curing time at 333.15 K is shortened from 3618 min at 323.15 K to 1243 min. In accordance with the Arrhenius equation, higher temperatures lead to an increase in the reaction rate constant. As a result, the curing reaction is expedited, thereby decreasing the time needed for curing.

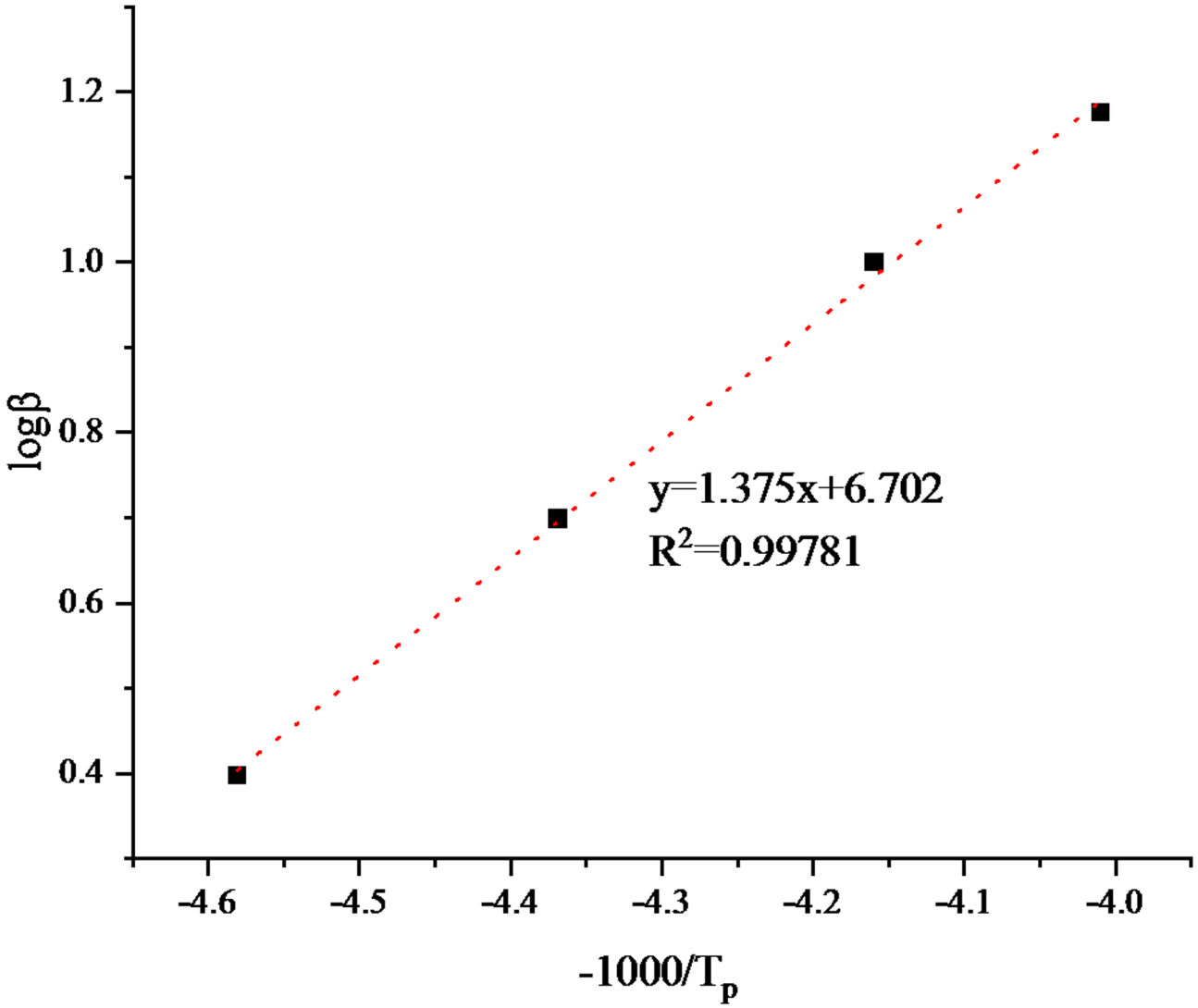

Fig. 7. Ozawa method for solving kinetic parameters.

	$\Delta E/(\mathrm{KJ{\cdot}mol^{-1}})$	n	R^2
Kissinger	22.439	0.8527	0.99662
Ozawa	25.031	0.9512	0.99781

Table 5. Kinetic parameters of the curing reaction process.

Curing occurs more rapidly at 348.15 K, with the process being completed in 473 min at a temperature of 348 K. The results are shown in Figs. 16 and 17. Higher temperatures further enhance molecular mobility and reaction rates. This enables the curing reaction to release a greater amount of heat and reach higher temperatures within a shorter time frame.

When the temperature was elevated, the discrepancies in temperature and degree of curing at various measurement points grew more substantial. This is because an increase in temperature accentuates the disparities in reaction rates at different positions, and it also intensifies the heat transfer and the lack of uniformity in the reaction process between the inner and outer parts of the samples.

During the later stage of the curing process, the shortening of the stage during which the temperature rises gradually is the principal factor contributing to the decrease in the curing time. This can be attributed to the rapid reaction rate at high temperatures. The heat accumulated in the initial stage of the swift reaction allows the system to attain higher temperatures more rapidly and enter the later curing stage. Additionally, in the later stage, the reaction rate becomes less sensitive to the influence of temperature, resulting in the shortening of this stage and, consequently, a reduction in the overall curing time. It can be clearly observed from Fig. 18 that under

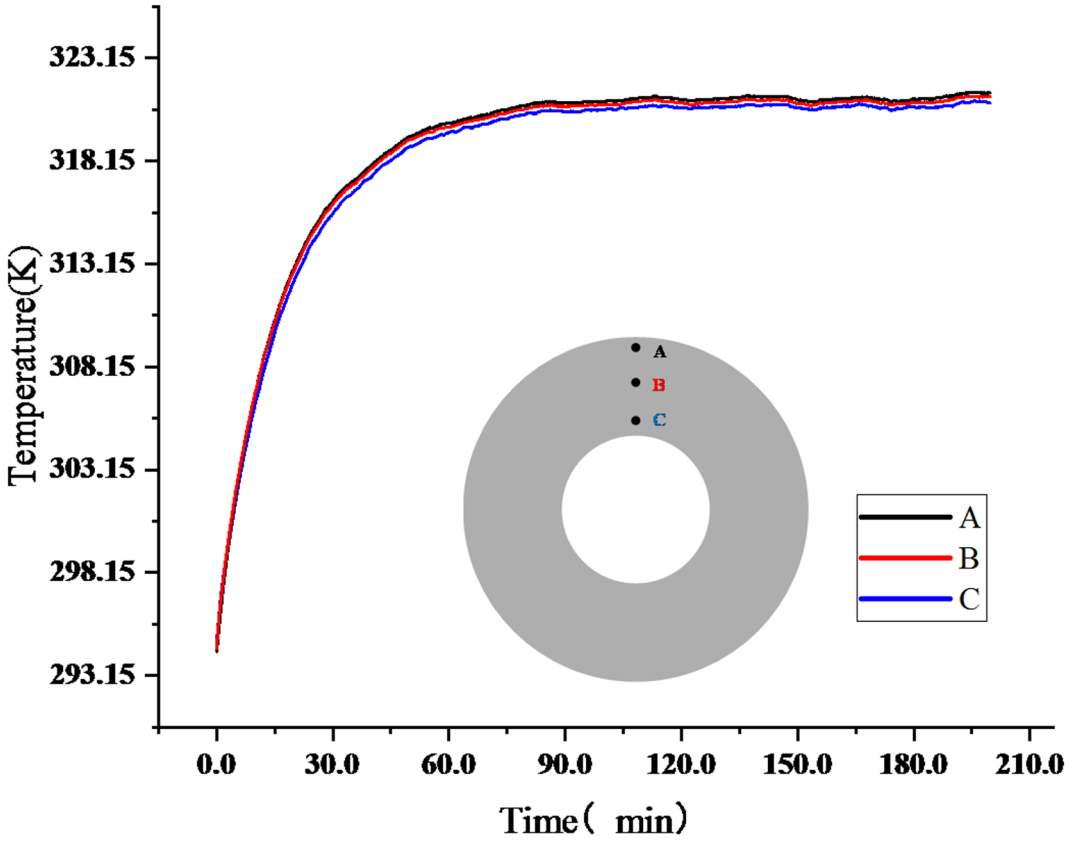

Fig. 8. Experimental testing of curing temperature-time curves at different nodes.

the condition of 348.15 K, the total curing time is only 473 min, which is a significant reduction compared to that under the other two temperature conditions in the experimental setup.

Conclusions

This study comprehensively investigated the curing kinetics and process of HTPB propellant through integrated experimental and theoretical approaches. Materials were carefully prepared, and systematic DSC experiments at varying heating rates captured reaction data. Theoretically, thermochemical and finite element models were developed, successfully revealing temperature and cure degree evolution patterns.

(1) Non-isothermal DSC analysis demonstrates that increased heating rates significantly shorten reaction time while raising initial, peak, and end temperatures. This occurs as accelerated heating disrupts molecular chain ordering, requiring higher transition temperatures to the elastomeric state. Kinetic parameters calculated via Kissinger and Ozawa methods further elucidate heating rate effects.
(2) Curing experiments show higher temperatures at the sample surface than core, with both ultimately reaching oven temperature. The three-stage curing process was accurately simulated, with < 5% maximum error versus experimental data. This validates the model's reliability in predicting temperature and cure degree profiles.

Building on validated curing kinetics models, this work paves the way for: (1) Rocket motor manufacturing through real-time cure monitoring during large-scale propellant casting to eliminate defects; (2) Next-generation propellants via model adaptation for AP/Al nanocomposites and sustainable HTPB alternatives; (3) Polymer-matrix armor systems by extending temperature-control protocols to impact-resistant flexible composites.

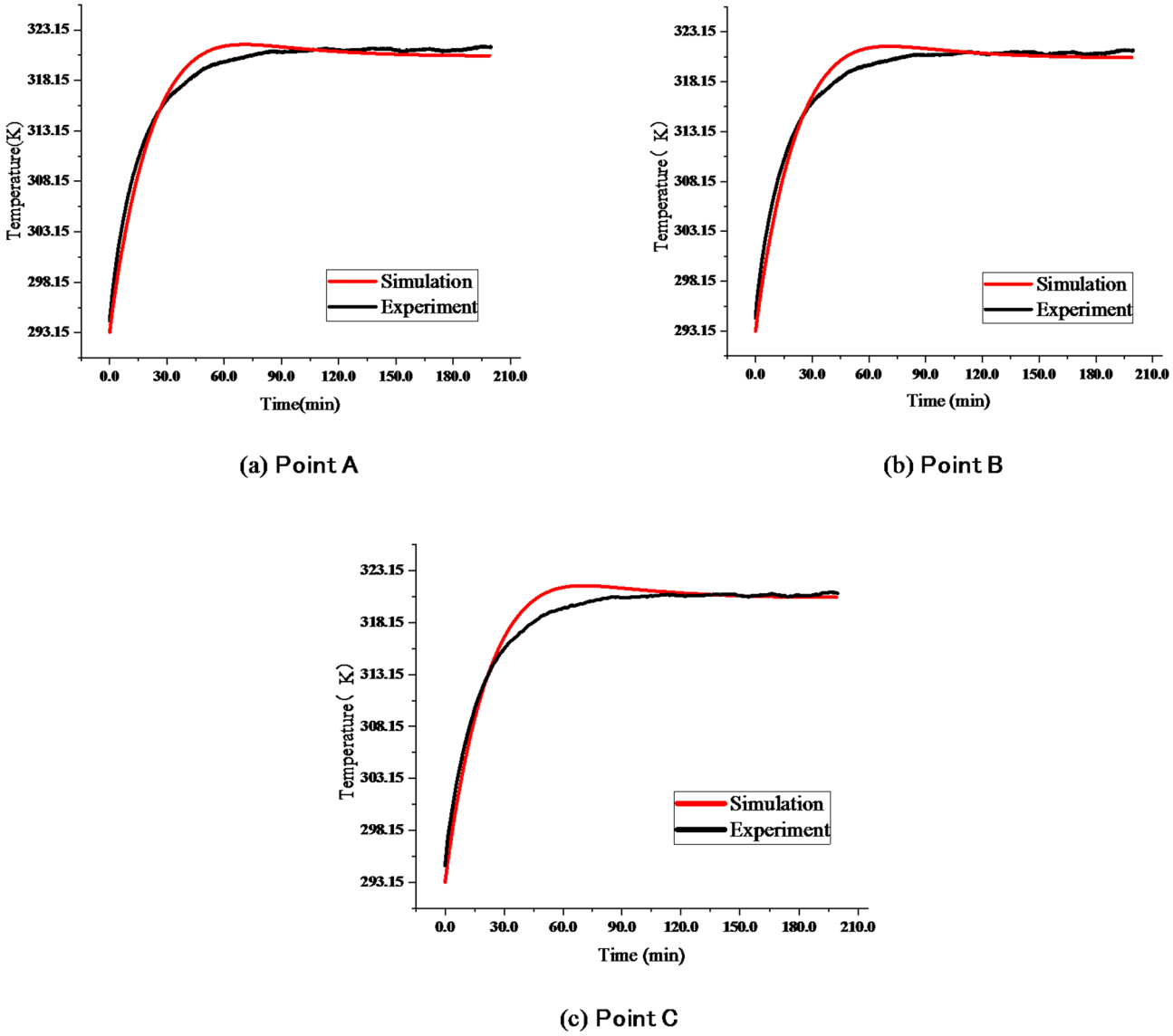

Fig. 9. Comparison of experimental and simulated temperature change curves.

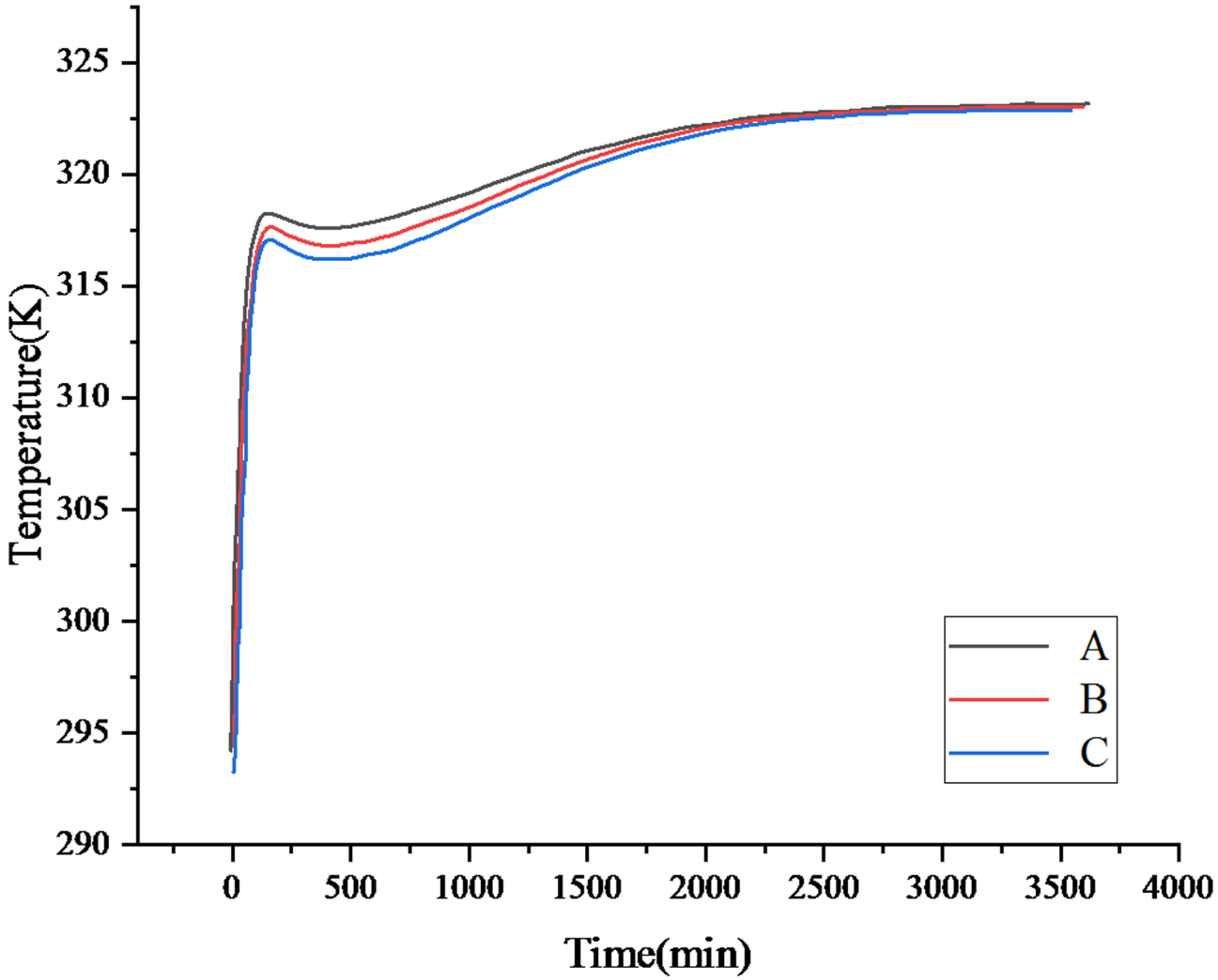

Fig. 10. Temperature curve at 323.15 K.

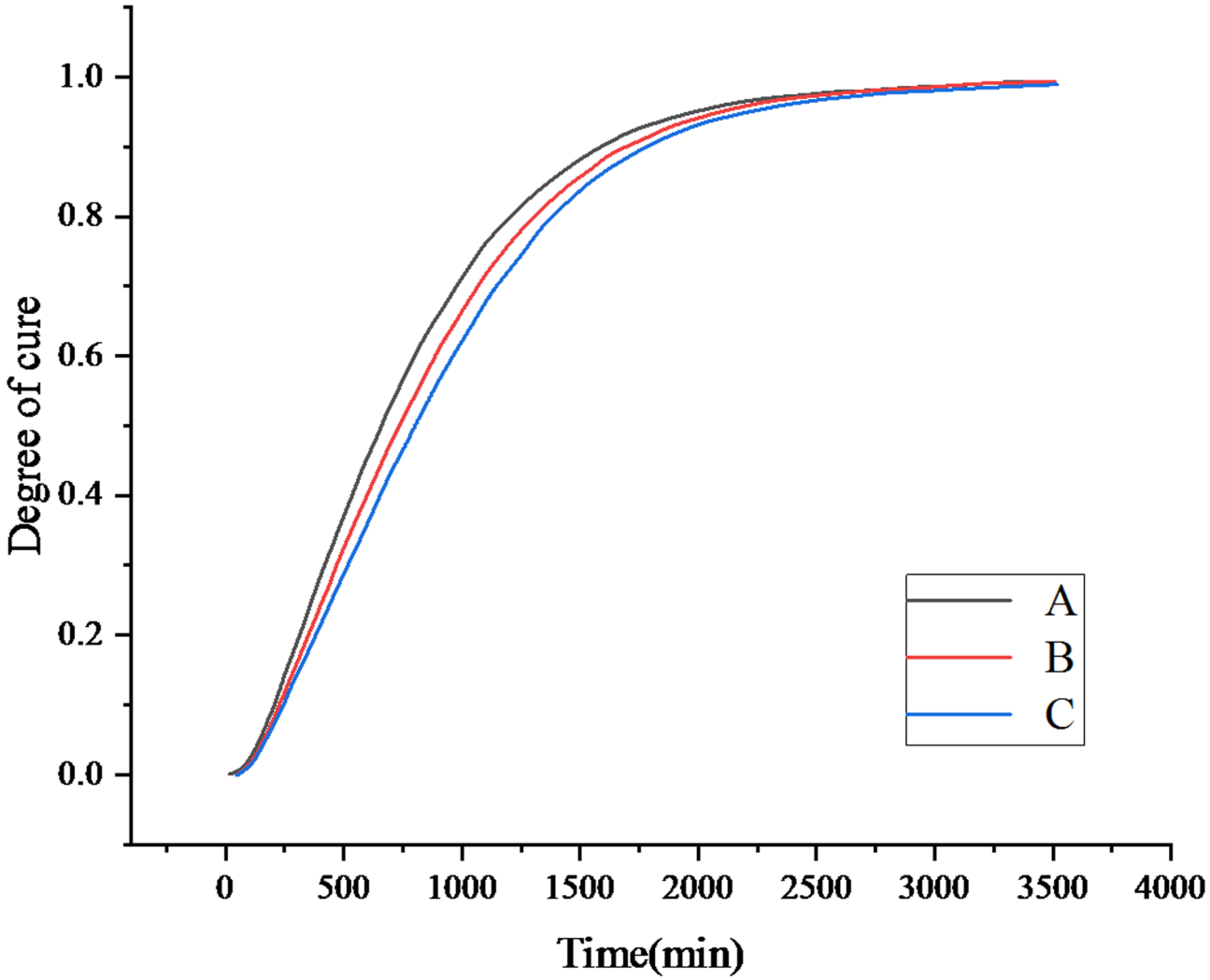

Fig. 11. Curing degree curve at 323.15 K.

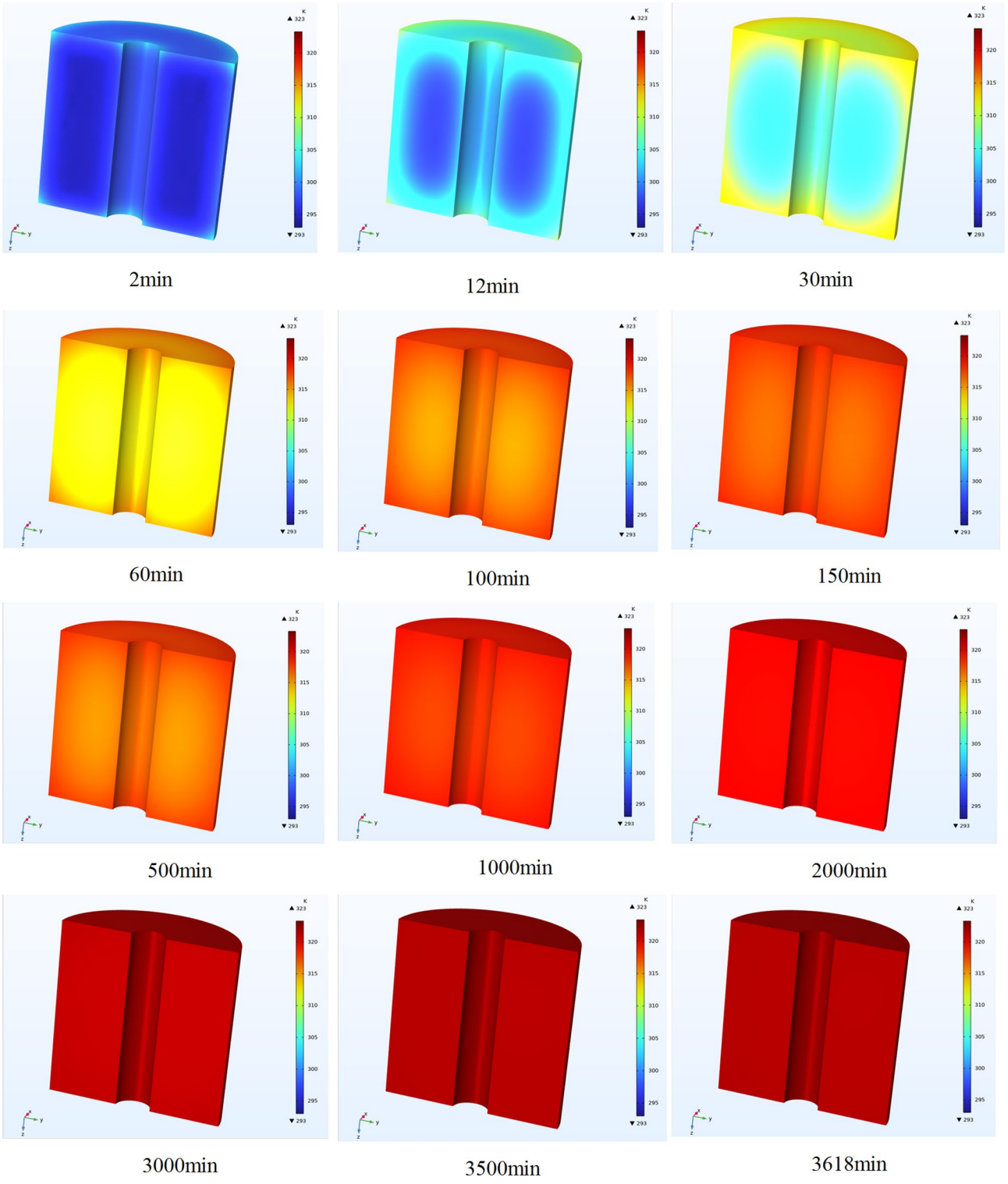

Fig. 12. Simulation of curing process at 323.15 K.

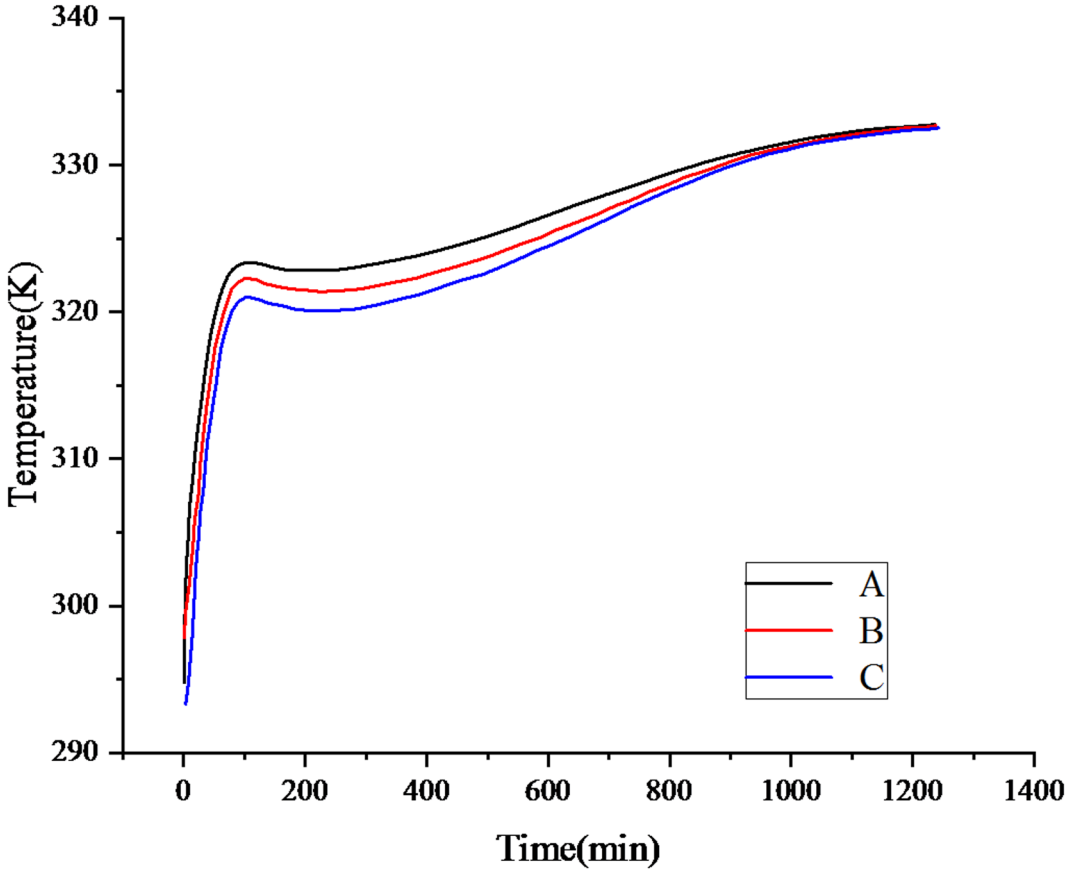

Fig. 13. Temperature curve at 333.15 K.

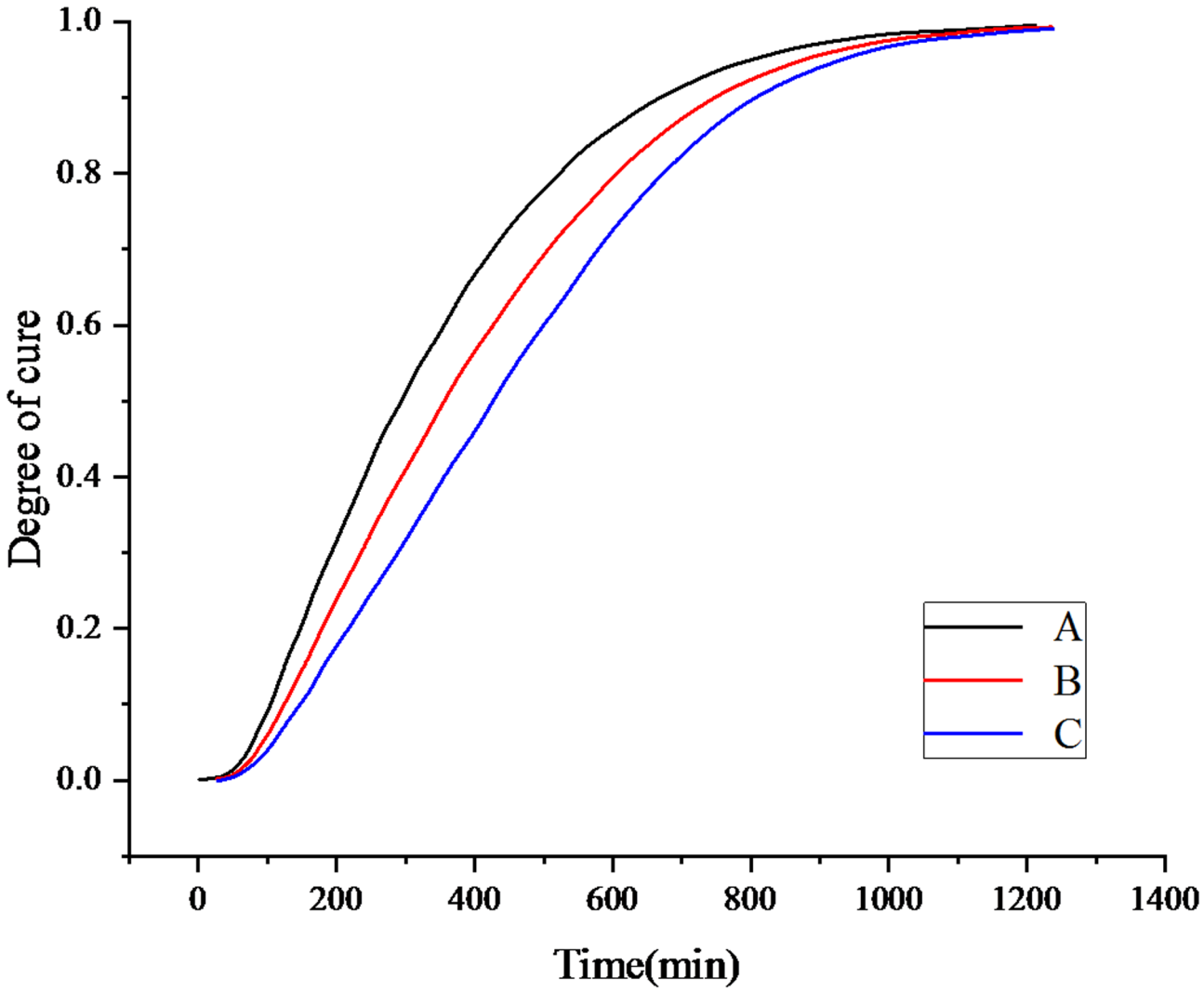

Fig. 14. Curing degree curve at 333.15 K.

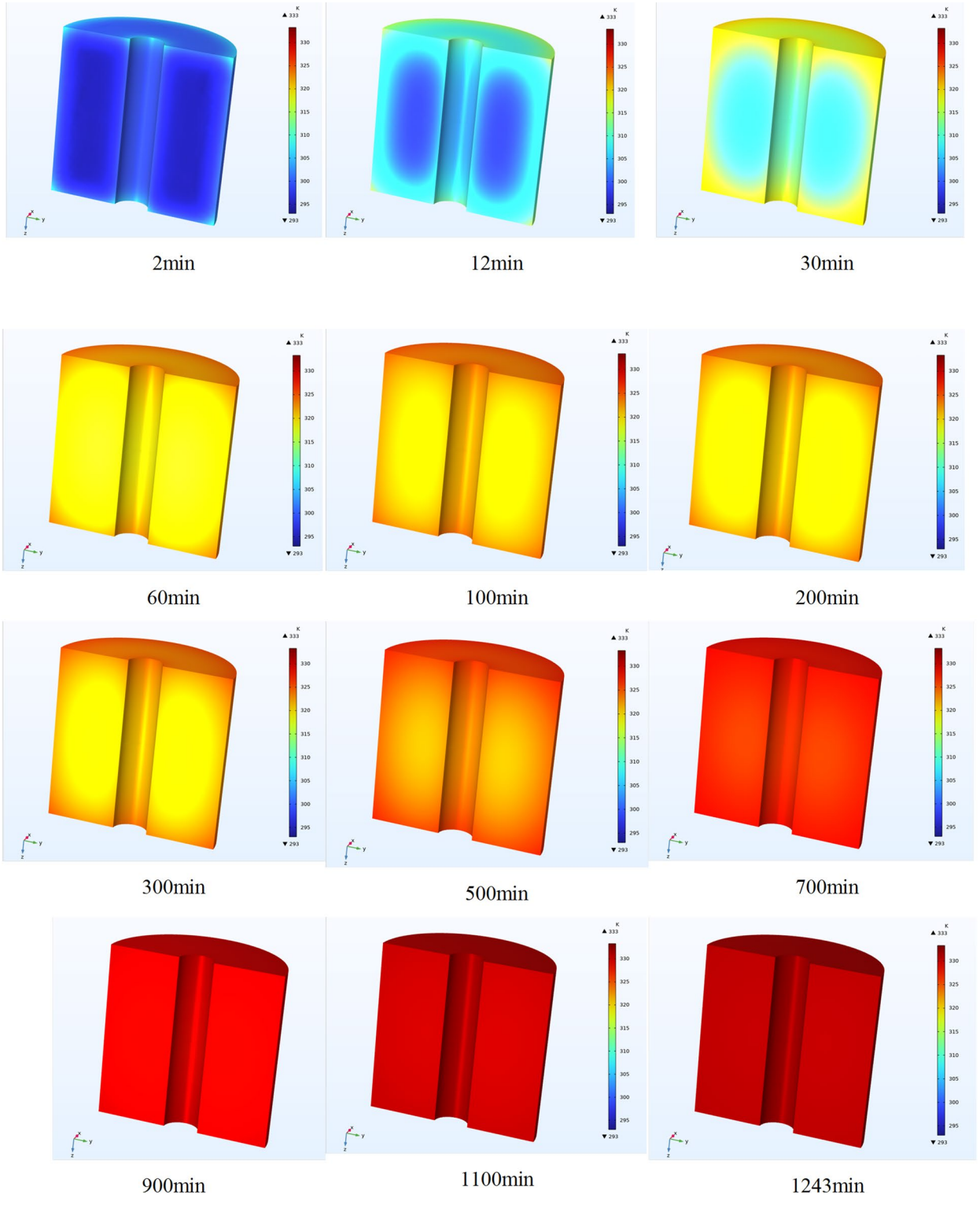

Fig. 15. Simulation of curing process at 333.15 K.

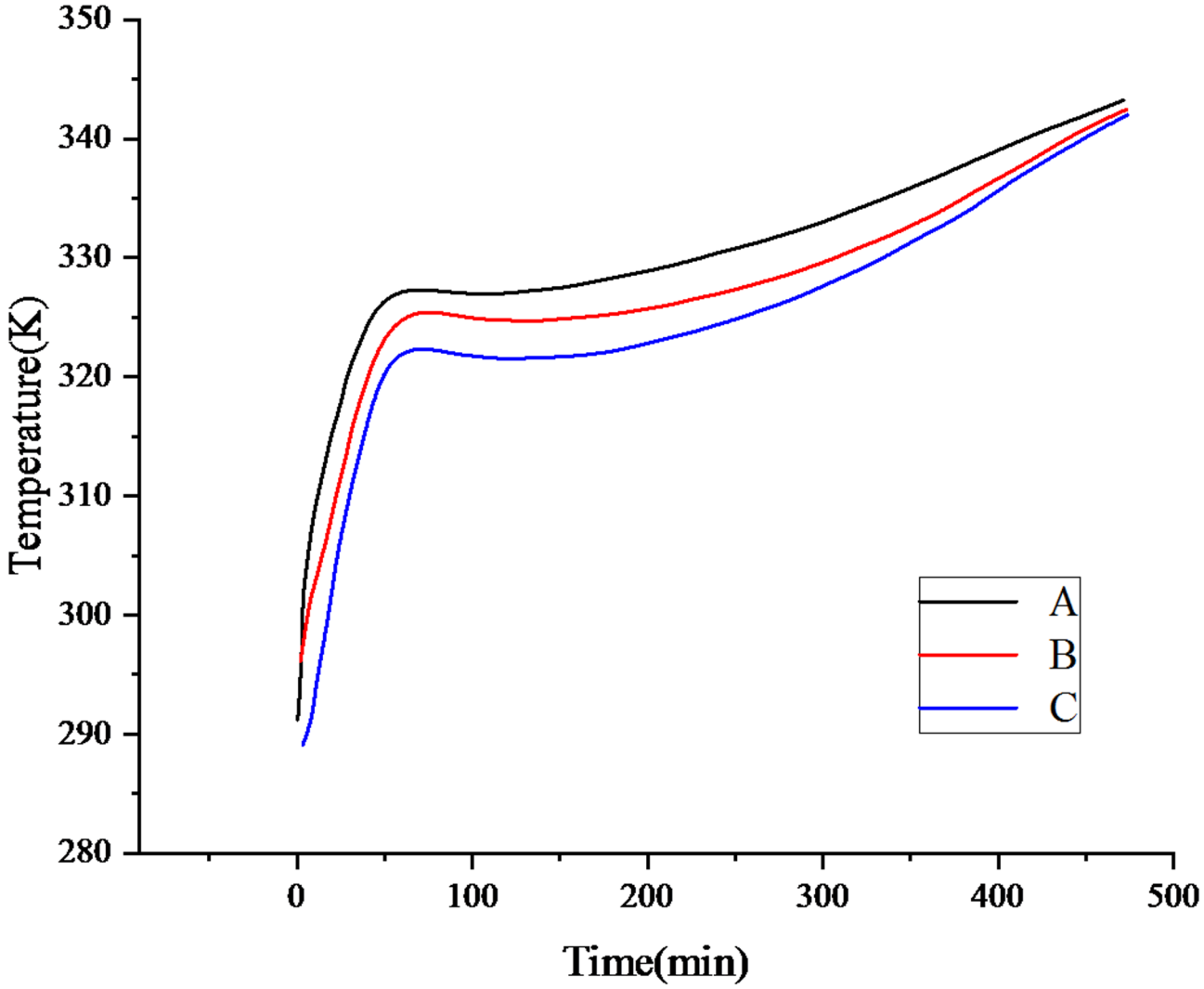

Fig. 16. Temperature curve at 348.15 K.

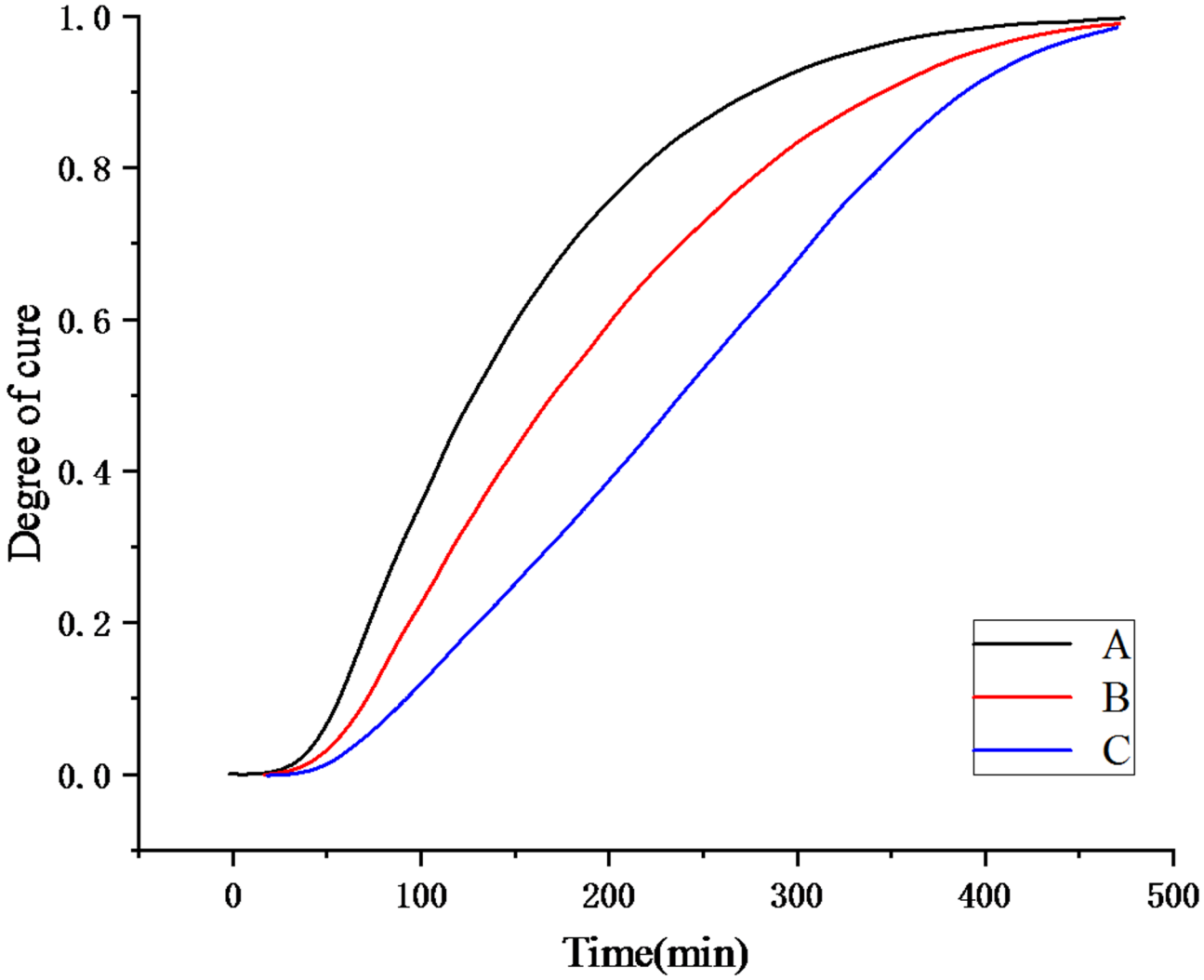

Fig. 17. Curing degree curve at 348.15 K.

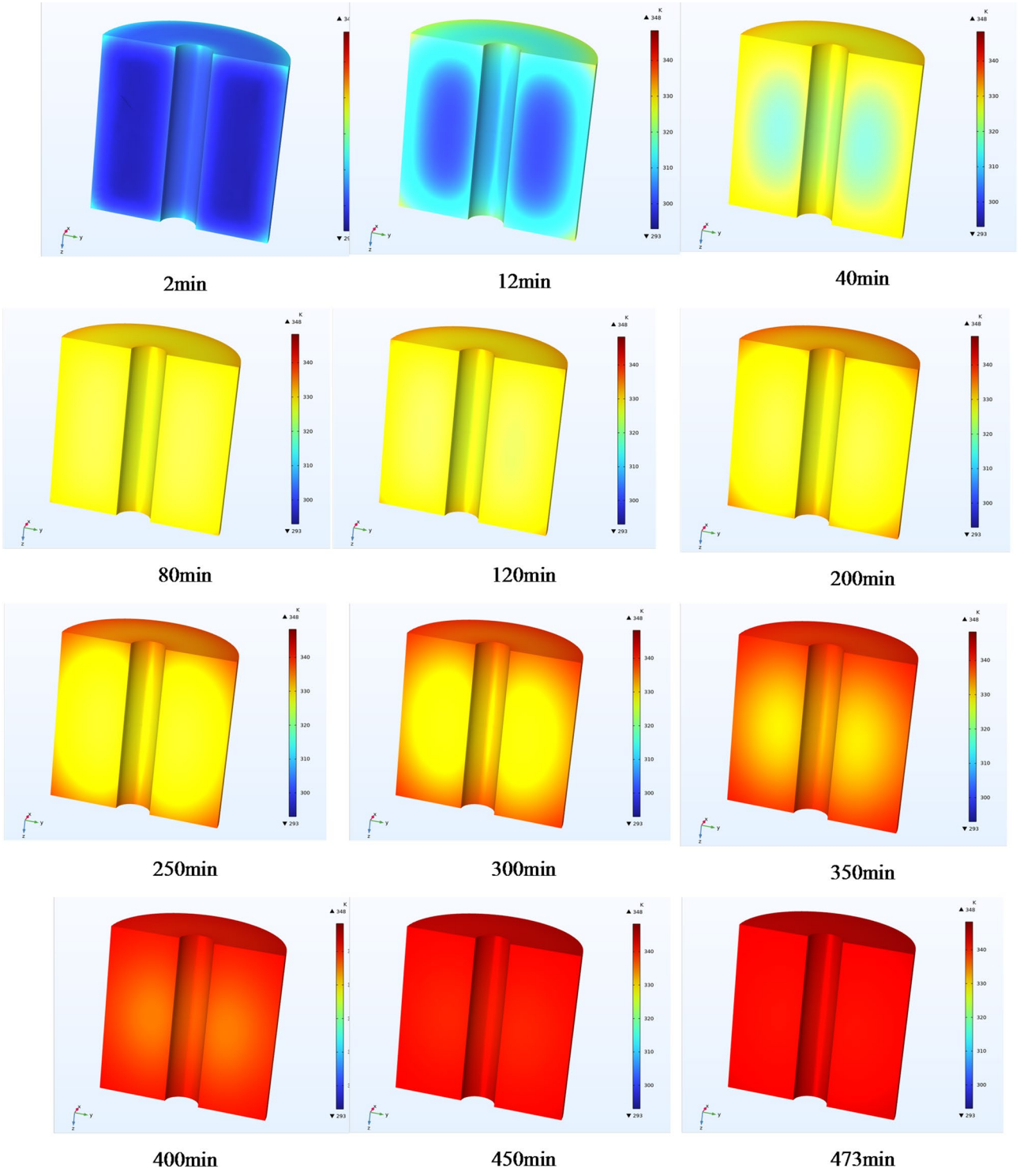

Fig. 18. Simulation of curing process at 348.15 K.

Data availability

Data Availability Statement: The data that support the findings of this study are available on request from the corresponding author, X.F., upon reasonable request.

Received: 16 April 2025; Accepted: 12 June 2025
Published online: 01 July 2025

References

1. Chaturvedi, S. & Dave, P. N. Solid propellants: AP/HTPB composite propellants. *Arab. J. Chem.* **12**, 2061–2068. https://doi.org/10.1016/j.arabjc.2014.12.033 (2019).
2. Jin, L., Qian, J., Fang, Q. Z., Hu, Q. W. & Yu, M. H. Study on mechanical properties of solid propellant NEPE. *Propellants Explos Pyrotech.* **48**, e202200338. https://doi.org/10.1002/prep.202200338 (2023).
3. Fu, X. & Fan, X. Curing reaction kinetics of HTPE polymer studied by simultaneous rheometry and FTIR measurements. *J. Therm. Anal. Calorim.* **125**, 977–982. https://doi.org/10.1007/s10973-016-5485-8 (2016).
4. Chan, M. L., Reed, R. & Ciaramitaro, D. A. Advances in soild propellant formulations. *Prog Astronaut. Aeronaut.* **185**, 185–206 (2000).
5. Xu, X. Q. & Yu, S. C. Transient temperature and stress analysis of propellant grains during cooling process after curing. *J. Solid Rocket Technol.* **27**, 183 (2004).
6. Moghimi Rad, H. et al. Numerical simulation of HTPB resin curing process using openfoam and study the effect of different conditions on its curing time. *Propellants, Explos., Pyrotech.* **46** (9), 1447–1457 (2021).
7. Chen, G. et al. Numerical and experimental study on the curing process of NEPE solid rocket propellant considering multi-physical field effects. *Case Stud. Therm. Eng.* **61**, 105124 (2024).
8. Liu, X., Xie, X., Zhou, D. & Wang, R. Numerical analysis of curing residual stress and strain in NEPE propellant grain. *Polymers* **15** (4), 1019. https://doi.org/10.3390/polym15041019 (2023).
9. Varghese, A. et al. Processability characteristics of hydroxy terminated polybutadienes. *Eur. Polymer J.* **32** (1), 79–83 (1996).
10. Lee, S. et al. Curing behavior of polyurethane as a binder for polymer-bonded explosives. *J. Ind. Eng. Chem.* **21**, 980–985 (2015).
11. Hui, M. et al. Kinetic studies on the cure reaction of hydroxyl-terminated polybutadiene based polyurethane with variable catalysts by differential scanning calorimetry. *e-Polymers* **17**, 89–94 (2017).
12. DeLuca, L. T. et al. Characterization of HTPB-based solid fuel formulations: performance, mechanical properties, and pollution. *Acta Astronaut.* **92** (2), 150–162 (2013).
13. Guo, J. et al. Kinetic research on the curing reaction of hydroxyl-terminated polybutadiene based polyurethane binder system via FT-IR measurements. *Coatings* **8**, 175 (2018).
14. Ma, H. et al. Catalyzed HTPB/HDI-trimer curing reactions and influence on pot life. *Coatings* **10**, 1073 (2020).
15. Ma, H. et al. The effect of single curing agents on the curing reactions of the HTPB-based binder system. *Coatings* **12**, 1090 (2022).
16. Zhang, X., Liu, Y., Chai, T., Ma, Z. & Jia, K. Curing reaction kinetics of the EHTPB-based PBX binder system and its mechanical properties. *Coatings* **10** (12), 1266 (2020).
17. Zhou, J. et al. The kinetics of the polyurethane moisture curing reaction: a combined experimental and DFT mechanistic study. *Reaction Chem. Eng.* **10** (1), 38–47 (2025).
18. Hoque, E. et al. Study of curing kinetics of 4-(dimethylsilyl) Butyl ferrocene grafted HTPB and effect of catalysts by differential scanning calorimetry. *Propellants, Explos., Pyrotech.* **49**, e202400110 (2024).
19. Korah Bina, C., Kannan, K. & Ninan, K. DSC study on the effect of isocyanates and catalysts on the HTPB cure reaction. *J. Therm. Anal. Calorim.* **78** (3), 753–760 (2004).
20. Chu, H. T. & Chou, J. H. Effect of cooling load on the safety factor of propellant grains. *J. Propuls. Power.* **29**, 27–33 (2013).
21. Cui, H., Tang, G. & Shen, Z. A three-dimensional viscoelastic constitutive model of solid propellant considering viscoelastic poisson's ratio and its implementation. *Eur. J. Mech. Solids.* **61**, 235–244 (2017).
22. Guo, X. et al. Effects of liner properties on the stress and strain alongliner/propellant interface in solid rocket motor. *Aerosp. Sci. Technol.* **58**, 594–600 (2016).
23. Yoon, J-S., Kim, K. & Seo, H-S. Computational modeling for cure process of carbon epoxy composite block. *Compos. Part. B: Eng.* **164**, 693–702 (2019).
24. Korah Bina, C., Kannan, K. & Ninan, K. DSC study on the effect of isocyanates and catalysts on the HTPB cure reaction. *J. Therm. Anal. Calorim.* **78**, 753–760. https://doi.org/10.1007/s10973-004-0442-3 (2004).
25. Zhao, L. & Hu, X. A variable reaction order model for prediction of curing kinetics of thermosetting polymers. *Polymer* **48**, 6125–6133. https://doi.org/10.1016/j.polymer.2007.07.067 (2007).
26. Franieck, E., Fleischmann, M., Hölck, O., Kutuzova, L. & Kandelbauer, A. Cure kinetics modeling of a high glass transition temperature epoxy molding compound (EMC) based on inline dielectric analysis. *Polymers* **13**, 1734 (2021).
27. Pang, W. et al. Thermal behavior and non-isothermal decomposition reaction kinetics of NEPE propellant with ammonium dinitramide. *Chin. J. Chem.* **28**, 1001–1003. https://doi.org/10.1002/cjoc.201090132 (2010).
28. Lim, A. C. R., Chin, B. L. F., Jawad, Z. A. & Hii, K. L. Kinetic analysis of rice husk pyrolysis using Kissinger-Akahira-Sunose (KAS) method. *Procedia Eng.* **148**, 1247–1251. https://doi.org/10.1016/j.proeng.2016.06.486 (2016).
29. Ozawa, T. Applicability of Friedman plot. *J. Therm. Anal.* **31**, 547–551. https://doi.org/10.1007/bf01914230 (1986).
30. Starink, M. J. The determination of activation energy from linear heating rate experiments: a comparison of the accuracy of isoconversion methods. *Thermochim Acta.* **404**, 163–176. https://doi.org/10.1016/s0040-6031(03)00144-8 (2003).
31. Crane, L. W., Dynes, P. J. & Kaelble, D. H. Analysis of curing kinetics in polymer composites. *J. Polym. Sci. Polym. Lett.* **11**, 533–540 (1973).

Author contributions

Author Contributions: Experiment test and analysis, Z.G., Y.W. (YuHeng Wu) ; software and simulation, M.C., Z.G., Y.W. (Yiliang Wang); writing original draft preparation, Y.W. (Yiliang Wang); Visualization, Y.W. (Yiliang Wang), S.Z.; Supervision, Z.G.X.F. ; Data Curation , Y.W. (YuHeng Wu) and R.R.; writing—review and editing, X.F. and H.L. All authors have read and agreed to the published version of the manuscript.

Declarations

Competing interests

The authors declare no competing interests.

Additional information

Correspondence and requests for materials should be addressed to X.F.

Reprints and permissions information is available at www.nature.com/reprints.

Publisher's note Springer Nature remains neutral with regard to jurisdictional claims in published maps and institutional affiliations.

Open Access This article is licensed under a Creative Commons Attribution-NonCommercial-NoDerivatives 4.0 International License, which permits any non-commercial use, sharing, distribution and reproduction in any medium or format, as long as you give appropriate credit to the original author(s) and the source, provide a link to the Creative Commons licence, and indicate if you modified the licensed material. You do not have permission under this licence to share adapted material derived from this article or parts of it. The images or other third party material in this article are included in the article's Creative Commons licence, unless indicated otherwise in a credit line to the material. If material is not included in the article's Creative Commons licence and your intended use is not permitted by statutory regulation or exceeds the permitted use, you will need to obtain permission directly from the copyright holder. To view a copy of this licence, visit http://creativecommons.org/licenses/by-nc-nd/4.0/.

© The Author(s) 2025